Wings of coherent backscattering from a disordered medium with large inhomogeneities

V. V. Marinyuk and D. B. Rogozkin
Moscow Engineering Physics Institute, National Research Nuclear University, Kashirskoe Shosse 31, 115409 Moscow, Russia
(Received 15 April 2011; published 20 June 2011)

We calculate the nondiffusive contribution to the intensity of coherent backscattering from a disordered medium composed of large-scale scatterers. The wings of the coherent backscattering cone are shown to be governed by short-path waves that experience small-angle multiple scattering before and after single scattering in the backward direction. For relatively large angles θ of deviation from the backward direction, $\theta > \lambda/l_{\rm tr}$ (λ is the wavelength of light, $l_{\rm tr}$ is the transport mean free path), the intensity falls off slower than θ^{-1} and is directly related to a law of single scattering through small angles. Our calculations are in good agreement with experimental data for large Mie spheres.

DOI: 10.1103/PhysRevE.83.066604 PACS number(s): 42.25.Dd, 42.25.Hz

I. INTRODUCTION

Interference between multiply scattered waves leads to striking phenomena, beyond the radiative transfer theory, like localization effects [1] and correlations in speckles [2]. The best known example of interference phenomena is weak localization, which is a direct consequence of the constructive interference between waves passing along the same paths in the opposite directions. The weak localization of light is observable as coherent backscattering (CB) from disordered systems [3]. Since the first experiments [3], a coherent enhancement of backscattering has been extensively studied in various disordered materials such as colloidal suspensions [4,5], powders [6,7], liquid crystals [8–10], biological tissues [11], etc.

Theoretical calculations of the CB intensity are based on summation of the most-crossed diagrams and can be reduced to solving the corresponding transfer equation [4,12–14]. Most of the theoretical results were derived within the diffusion approximation and permit one to describe the backscattering intensity in a narrow cone around the exact backward direction, $\theta < \lambda/l_{\rm tr}$. For arbitrary θ, there are only numerical calculations (see, e.g., [14,15]).

The angular width of the backscattering cone depends on the turbidity of the sample. This allows one to extract the values of transport coefficients of the medium (e.g., the transport mean free path) directly from experimental data (see, e.g., [4,7,10]).

Not much is known about the angular dependence of intensity at the wings ($\theta > \lambda/l_{\rm tr}$) of the CB cone. As analysis shows, for $\theta > \lambda/l_{\rm tr}$, intensity of CB is governed by relatively short paths of wave propagation (their length is less than $l_{\rm tr}$). The short-path contribution is of particular importance for media with large-scale scatterers (size a is greater than wavelength λ). In this case, transport mean free path $l_{\rm tr}$ appears to be large as compared to the mean free path l, $l_{\rm tr} \gg l$, and the CB intensity at $\theta > \lambda/l_{\rm tr}$ results from multiple scattering through small angles before and after single scattering through a large angle, that is, in accordance with the "forward-scatter single-backscatter" mechanism described in [16].

Considerable interest in turbid media with large-scale inhomogeneities is due to numerous applications. Examples of such systems are colloidal suspensions containing large Mie particles [5], biological tissues [11,17], random media with long-range correlations of inhomogeneities such as liquid crystals [8–10,18], fractal structures [19,20], and matter in the vicinity of the phase transition point [21].

In this paper, we present the results of calculations of intensity at the wings of the CB cone, $\theta > \lambda/l_{\rm tr}$. The intensity is shown to fall off, as θ increases, slower than it follows from the diffusion theory [4,13]. Using the power-law type of the scattering phase function $p(\vartheta) \sim 1/\vartheta^{\alpha}$, we find the interrelation between the shape of the backscattering cone wings and the single scattering law. The demarcation between our results and the diffusion theory [4,13] are illustrated for the important examples of power-law phase functions with $\alpha = 3$ and $\alpha = 2$. These cases correspond, respectively, to the Henyey-Greenstein phase function [22,23] and the scattering by liquid crystals [18,21]. The range of validity for the second-order scattering approximation is also established. Our calculations of the CB intensity are carried out within the scalar theory of wave propagation. For comparison with experimental data, the results obtained are generalized with allowance for the polarization state of light. The calculated angular dependence of the backscattering intensity is shown to be in good agreement with experimental data [5] for large Mie spheres.

II. INTENSITY OF COHERENT BACKSCATTERING WITHIN THE "FORWARD-SCATTER SINGLE-BACKSCATTER" APPROXIMATION

Let us consider CB of a plane wave incident on a turbid medium with large-scale inhomogeneities. The medium is assumed to occupy the half space $z > 0$, and the z axis coincides with the inward normal to the surface.

According to the diffusion theory of CB (see, e.g., [4,13]), the flux of backscattered waves is generated over paths $s > l_{\rm tr}$ as a result of numerous events of scattering through small angles. Transport mean free path $l_{\rm tr}$ is a distance over which an initially directional flux of radiation transforms to an isotropic one. In the case of large scattering inhomogeneities, transport mean free path $l_{\rm tr}$ is much greater than mean free path l ($l_{\rm tr} = l/(1 - \langle\cos\vartheta\rangle) \gg l$, where $\langle\cos\vartheta\rangle$ is the mean cosine of the single-scattering angle [22]).

The diffusion theory does not describe the contribution from relatively short trajectories of wave propagation, $s < l_{\rm tr}$. The contribution from short paths $s < l_{\rm tr}$ to the intensity of backscattering is governed by the mechanism proposed by De Wolf [16]. For $s < l_{\rm tr}$, the small-angle multiple scattering can not give rise to the reflected flux. The reflected flux is only due to single scattering through a large angle (of the order of π). An analogous mechanism was discussed in many works in the context of enhancement of reflection from objects observed through a turbulent medium (see, e.g., [24] and references therein).

In accordance with general ideas (see, e.g., [4,13]), for angles of deviation from the backward direction $\theta < \lambda/\sqrt{l_{\rm tr}s}$, the intensity of backscattering is governed by the trajectories longer than s. Therefore, the diffusion theory describes only the peak ($\theta < \lambda/l_{\rm tr}$) of the backscattering cone, whereas the wings of the angular dependence of intensity ($\theta > \lambda/l_{\rm tr}$) are described by the process of multiple scattering along short ($s < l_{\rm tr}$) trajectories which is accompanied by deflection through a large angle in one of scattering events.

In order to find the contribution from relatively short trajectories to the intensity of CB, it is necessary to calculate the sum of the most-crossed diagrams, each involving one scattering through a large angle [25,26] (such a diagram is actually shown in Fig. 1). Using the standard technique for calculating diagrams [4,13,22], we can derive the following expression for the intensity of CB:

$$J_{\rm c}(\boldsymbol{\theta}) = n\int_0^\infty {\rm d}z\Bigg[\int_{\Omega_{1z}>0} {\rm d}\boldsymbol{\Omega}_1 \int_{\Omega_{2z}>0} {\rm d}\boldsymbol{\Omega}_2 I_{\mathbf{q}}(z,\boldsymbol{\Omega}_1|\boldsymbol{\Omega}_0) \times \frac{{\rm d}\sigma}{{\rm d}\Omega}(-\boldsymbol{\Omega}_1\boldsymbol{\Omega}_2) I_{-\mathbf{q}}(z,\boldsymbol{\Omega}_2|\boldsymbol{\Omega}_0) - \frac{1}{\Omega_{0z}^2}\exp\left\{\frac{-2n\sigma_{\rm tot}z}{\Omega_{0z}}\right\}\frac{{\rm d}\sigma}{{\rm d}\Omega}(-\boldsymbol{\Omega}_0\boldsymbol{\Omega}_0)\Bigg], \qquad (1)$$

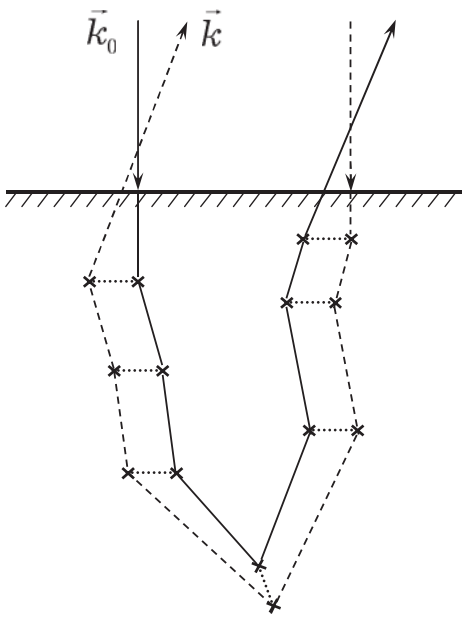

FIG. 1. Interference between reciprocal light paths in wave backscattering.

where $\boldsymbol{\theta} = \mathbf{q}/k_0$ is the angle of deviation from the backward direction, $\mathbf{q} = (\mathbf{k}+\mathbf{k}_0)_\parallel$, $k_0 = 2\pi/\lambda$, $\mathbf{k}_0$ and $\mathbf{k}$ are the wave vectors of the incident and outgoing waves, $\mathbf{k}_{0\parallel}$ and $\mathbf{k}_\parallel$ are the components that are parallel to the surface of the medium, $\boldsymbol{\Omega}_0 = \mathbf{k}_0/k_0$, n is the number of scattering particles per unit volume, ${\rm d}\sigma/{\rm d}\Omega$ is the differential cross section of single scattering, $\sigma_{\rm tot} = \sigma + \sigma_{\rm a}$ is the total cross section of interaction, and σ and $\sigma_{\rm a}$ are the cross sections of elastic scattering and absorption, respectively. The single-scattering contribution which has no relation to the interference part of the intensity is excluded from Eq. (1) (see the last term in the square brackets).

Quantity $I_{\mathbf{q}}(z,\boldsymbol{\Omega}|\boldsymbol{\Omega}_0)$ entering into Eq. (1) is the ladder propagator which describes the small-angle multiple wave scattering before and after deflection through a large angle (see Fig. 1). This quantity has a simple physical meaning. The function $I_{\mathbf{q}}(z,\boldsymbol{\Omega}|\boldsymbol{\Omega}_0)$ is given by

$$I_{\mathbf{q}}(z,\boldsymbol{\Omega}|\boldsymbol{\Omega}_0) = \int {\rm d}^2\boldsymbol{\rho}\exp({\rm i}\mathbf{q}\boldsymbol{\rho}) I(z,\boldsymbol{\rho},\boldsymbol{\Omega}|\boldsymbol{\Omega}_0), \qquad (2)$$

where $I(z,\boldsymbol{\rho},\boldsymbol{\Omega}|\boldsymbol{\Omega}_0)$ is the intensity of radiation at the point $\mathbf{r} = (z,\boldsymbol{\rho})$ in the direction $\boldsymbol{\Omega}$, for waves being emitted in the direction $\boldsymbol{\Omega}_0$ by a point source located at the boundary ($z_0 = 0, \boldsymbol{\rho}_0 = 0$). The intensity of radiation obeys the radiative transfer equation

$$\left(\boldsymbol{\Omega}\frac{\partial}{\partial\mathbf{r}} + n\sigma_{\rm tot}\right) I(\mathbf{r},\boldsymbol{\Omega}|\boldsymbol{\Omega}_0) = n\int {\rm d}\boldsymbol{\Omega}'\frac{{\rm d}\sigma}{{\rm d}\Omega}(\boldsymbol{\Omega}'\boldsymbol{\Omega}) I(\mathbf{r},\boldsymbol{\Omega}'|\boldsymbol{\Omega}_0), \qquad (3)$$

with the boundary condition

$$I(z=0,\boldsymbol{\rho},\boldsymbol{\Omega}|\boldsymbol{\Omega}_0) = \delta(\boldsymbol{\rho})\delta(\boldsymbol{\Omega}-\boldsymbol{\Omega}_0).$$

Below we do not consider the effects caused by absorption in the medium as well as by an oblique incidence of waves on the surface. Following are the results related to normal incidence ($\Omega_{0z} = 1$) and the medium with no absorption ($\sigma_{\rm a} = 0$).

As follows from Eq. (1) the angular distribution $J_{\rm c}(\boldsymbol{\theta})$ is expressed in terms of the scattering cross section averaged over angles around the backward direction within the cone with the width that is governed by the angular dependence of the $I_{\mathbf{q}}$ functions appearing in Eq. (1). The effective width of the cone exceeds at least the characteristic value of single-scattering angle. Neglecting the effects caused by the fine ($\Delta\vartheta \sim \lambda/a$) structure of the angular dependence of the differential cross section ${\rm d}\sigma/{\rm d}\Omega$ in the vicinity of the backward direction [14] and assuming that the averaged ${\rm d}\sigma/{\rm d}\Omega$ is a smooth function of the backscattering angle, we can write Eq. (1) in the more simple form [26]

$$J_{\rm c}(\theta) = n\sigma_{\rm b}\int_0^\infty {\rm d}z[|I_q(z)|^2 - \exp(-2n\sigma z)], \qquad (4)$$

where $\sigma_{\rm b} = \overline{\frac{{\rm d}\sigma}{{\rm d}\Omega}}(-1)$ is the backscattering cross section averaged over the angular scale exceeding λ/a and $I_q(z) = \int_{\Omega_z>0} {\rm d}\boldsymbol{\Omega}\, I_q(z,\boldsymbol{\Omega}|\boldsymbol{\Omega}_0)$. Analogous formula expressed in terms of the mutual coherence function was derived in [25].

The function $I_q(z)$ can be found from the well-known solution of the transfer equation (3) within the small-angle approximation [22]. According to [22] $I_q(z)$ has the form

$$I_q(z) = \exp\left(-\frac{1}{l}\int_0^z \mathrm{d}z'[1-\hat{p}(qz')]\right), \tag{5}$$

where $l = (n\sigma)^{-1}$ is the mean free path. Quantity $\hat{p}(\omega)$ is governed by the differential cross section of scattering through small angles. Defining the phase function as [22]

$$p = \frac{1}{\sigma}\frac{\mathrm{d}\sigma}{\mathrm{d}\Omega},$$

we can present $\hat{p}(\omega)$ in the form

$$\hat{p}(\omega) = \int_0^\infty 2\pi p(\vartheta)\mathrm{J}_0(\omega\vartheta)\vartheta\,\mathrm{d}\vartheta, \tag{6}$$

where $p(\vartheta)$ is the phase function of scattering through small angles, $\mathrm{J}_0(x)$ is the Bessel function [27]. Equation (6) is the small-angle limit of more general formula

$$\hat{p}(\omega) = \int_0^\pi 2\pi p(\vartheta)\mathrm{P}_\omega(\cos\vartheta)\sin\vartheta\,\mathrm{d}\vartheta, \tag{7}$$

where $\mathrm{P}_\omega(\cos\vartheta)$ is the Legendre polynomial [27]. Equation (6) follows from Eq. (7) if we take advantage of asymptotic formula $\mathrm{P}_\omega(\cos\vartheta) \approx \mathrm{J}_0(\omega\vartheta)$ and substitute infinity for π in the upper limit of integrating over ϑ.

Substituting Eq. (5) into Eq. (4), we find the nondiffusion contribution to the CB intensity. Equations (4) and (5) hold for relatively large angles of deviation from the backward direction, $\theta = q/k_0 > 1/k_0 l_{\mathrm{tr}}$, and so describe the wings around the peak of CB.

III. WINGS OF THE CB INTENSITY

Consider the specific features of the intensity which are associated with wave propagation along relatively short ($s < l_{\mathrm{tr}}$) paths. We restrict our analysis to the case where the scattering phase function decreases with angle ϑ in accordance with a power law,

$$p(\vartheta) \sim 1/\vartheta^\alpha. \tag{8}$$

To model behavior of Eq. (8) we take advantage of the following parametrization [28]

$$p(\vartheta) = \frac{p_\alpha}{2\pi[\vartheta_0^2 + 2(1-\cos\vartheta)]^{\alpha/2}}, \tag{9}$$

where ϑ_0 is the characteristic angle of single scattering. For large particles, the forward scattering dominates and $\vartheta_0 \ll 1$. Normalization factor p_α appearing in Eq. (9) approximates $p_\alpha = (\alpha-2)\vartheta_0^{\alpha-2}$ $(\alpha > 2)$ and $p_\alpha = 1/\ln(2/\vartheta_0)$ $(\alpha = 2)$. The relation between the mean cosine of the single-scattering angle and ϑ_0 has the form

$$1 - \langle\cos\vartheta\rangle = \begin{cases} \vartheta_0^2\ln(1/\vartheta_0), & \alpha = 4, \\ \frac{2(\alpha-2)}{4-\alpha}\left(\frac{\vartheta_0}{2}\right)^{\alpha-2}, & 2 < \alpha < 4, \\ \frac{1}{\ln(2/\vartheta_0)}, & \alpha = 2. \end{cases} \tag{10}$$

Parametrization of the form (9) unifies a number of scattering models. For $\alpha = 4$, Eq. (9) describes scattering of light by weakly refracting inhomogeneities [22,29,30], in particular, by a medium with the Booker-Gordon correlation function [22]. Equation (9) with $\alpha = 3$ corresponds to the Henyey-Greenstein phase function that is used very widely to model scattering of light in natural media [17,22,23].

Of particular interest is the case of $\alpha = 2$. This case corresponds to scattering of light by liquid crystals [8–10,18] and by substances in the vicinity of the phase transition point [21]. For $\alpha = 2$, $\vartheta_0 \sim 1/k_0 a$, where a is the radius of correlation between inhomogeneities of the refractive index (i.e., the correlation length or the size of an ordered region [18,21]).

The small-angle form of Eq. (9) at $\alpha > 2$ is given by

$$p(\vartheta) = \frac{\alpha-2}{2\pi}\frac{\vartheta_0^{\alpha-2}}{\left(\vartheta_0^2+\vartheta^2\right)^{\alpha/2}}. \tag{11}$$

For Eq. (11), the $\hat{p}$ function (6) is equal to

$$\hat{p}(\omega) = \frac{2}{\Gamma(\alpha/2-1)}\left(\frac{\omega\vartheta_0}{2}\right)^{\alpha/2-1}\mathrm{K}_{\alpha/2-1}(\omega\vartheta_0), \tag{12}$$

where $\Gamma(x)$ is the Gamma function and $\mathrm{K}_\nu(x)$ is the Macdonald function [27]. Substituting Eq. (12) into Eqs. (4) and (5), we obtain

$$J_{\mathrm{c}}(\theta) = \frac{\sigma_{\mathrm{b}}}{\sigma}F(ql\vartheta_0), \tag{13}$$

where

$$\sigma_{\mathrm{b}} = \frac{\alpha-2}{8\pi}\sigma\left(\frac{\vartheta_0}{2}\right)^{\alpha-2} \tag{14}$$

is the backscattering cross section for phase function (9) and

$$F(x) = \int_0^\infty \mathrm{d}\zeta\,\mathrm{e}^{-2\zeta} \times\left[\exp\left(\frac{4}{\Gamma(\alpha/2-1)}\int_0^\zeta \mathrm{d}\zeta'\right.\right. \times\left.\left.\left(\frac{x\zeta'}{2}\right)^{\alpha/2-1}\mathrm{K}_{\alpha/2-1}(x\zeta')\right) - 1\right]. \tag{15}$$

The angular dependence of $J_{\mathrm{c}}(\theta)$ turns out to be a universal function of argument $ql\vartheta_0 = k_0\theta l\vartheta_0$.

For small values of the argument, $\theta < 1/k_0 l\vartheta_0$, expanding the K function in powers of $x\zeta'$, we arrive at a simple asymptotic formula,

$$J_{\mathrm{c}}(\theta) = c_\alpha\frac{\sigma_{\mathrm{b}}}{\sigma_{\mathrm{tr}}}(k_0 l_{\mathrm{tr}}\theta)^{-\frac{\alpha-2}{\alpha-1}}, \qquad c_\alpha = \Gamma\left(\frac{\alpha}{\alpha-1}\right)\left[\frac{(\alpha-1)(\alpha/2-1)\Gamma(\alpha/2)}{\Gamma(3-\alpha/2)}\right]^{\frac{1}{\alpha-1}}. \tag{16}$$

Equation (16) is valid at $2 < \alpha < 4$. For $\alpha > 4$, the CB intensity decreases as $J_{\mathrm{c}}(\theta) \sim 1/\theta^{2/3}$.

At large values of the argument $(\theta > 1/k_0 l\vartheta_0)$ Eqs. (13) and (15) lead to

$$J_{\mathrm{c}}(\theta) = \frac{(\alpha-2)\Gamma[(\alpha-1)/2]}{2^{\alpha+1}\sqrt{\pi}\Gamma(\alpha/2-1)}\frac{\vartheta_0^{\alpha-3}}{k_0 l\theta}. \tag{17}$$

Equation (17) corresponds to the second-order scattering contribution (see below). When putting $\alpha = 3$ in Eqs. (16) and (17), we arrive at results as in [25,26].

To calculate the $\hat{p}$ function for $\alpha = 2$ we take advantage of Eq. (7) [formula (6) overestimates the value of intensity due to the logarithmic divergence at $\omega = 0$]. Then the $\hat{p}$ function takes the form

$$\hat{p}(\omega) = \frac{\mathrm{Q}_\omega\left(1 + \vartheta_0^2/2\right)}{\ln(2/\vartheta_0)}, \tag{18}$$

where $\mathrm{Q}_\omega(x)$ is the Legendre function of the second kind [27]. For $\vartheta_0 \ll 1$, $\mathrm{Q}_\omega(1 + \vartheta_0^2/2) = \mathrm{K}_0[(\omega + \gamma)\vartheta_0]$, where $\gamma = 0.5615\ldots$, and $J_\mathrm{c}(\theta)$ takes the form

$$J_\mathrm{c}(\theta) = \frac{1}{8\pi \ln(2/\vartheta_0)} \int_0^\infty \mathrm{d}\zeta\, \mathrm{e}^{-2\zeta} \times \left[\exp\left(\frac{2}{\ln(2/\vartheta_0)} \int_0^\zeta \mathrm{d}\zeta'\, \mathrm{K}_0[(ql\zeta' + \gamma)\vartheta_0]\right) - 1\right]. \tag{19}$$

Within interval $1/k_0 l_\mathrm{tr} < \theta < 1/k_0 l \vartheta_0$, integral (19) can be estimated by

$$J_\mathrm{c}(\theta) = \frac{1}{16\pi \ln(k_0 l_\mathrm{tr}\theta)}. \tag{20}$$

At large angles, $\theta > 1/k_0 l \vartheta_0$, intensity $J_\mathrm{c}(\theta)$ falls off as

$$J_\mathrm{c}(\theta) = \frac{1}{16 \ln^2(2/\vartheta_0)\vartheta_0 k_0 l\theta}. \tag{21}$$

From Eqs. (17) and (21) it follows that universal law $J_\mathrm{c}(\theta) \sim 1/\theta$ is valid for large deviations from the backward direction ($\theta \gg 1/k_0 l \vartheta_0$, where ϑ_0 is the characteristic angle of single scattering). In this case the leading contribution to the angular dependence of intensity is governed by second-order scattering. To calculate $J_\mathrm{c}^{(2)}(\theta)$, it is sufficient to retain the linear term in expansion of Eq. (5) in powers of the $\hat{p}$ function. As a result, we obtain

$$J_\mathrm{c}^{(2)}(\theta) = n\sigma_\mathrm{b} \int_0^\infty \mathrm{d}z\, \hat{p}(qz)\mathrm{e}^{-2z/l} = \frac{\sigma_\mathrm{b}}{\sigma} \int_0^\infty \frac{2\pi p(\vartheta)\vartheta\, \mathrm{d}\vartheta}{\sqrt{4 + (ql\vartheta)^2}}. \tag{22}$$

Note that Eq. (22) is the small-angle version of the exact expression for $J_\mathrm{c}^{(2)}(\theta)$ which is as follows:

$$J_\mathrm{c}^{(2)}(\theta) = \int_0^{\pi/2} \frac{2\pi p(\vartheta) p(\pi - \vartheta) \sin\vartheta\, \mathrm{d}\vartheta}{\sqrt{(1 + \cos\vartheta)^2 + (ql\sin\vartheta)^2}}. \tag{23}$$

For large scatterers ($1 - \langle\cos\vartheta\rangle \ll 1$) Eqs. (22) and (23) yield equal results. According to Eqs. (22) and (23), the dependence $J_\mathrm{c} \sim 1/\theta$ gets universally valid as angle θ increases.

It is instructive to compare Eqs. (13)–(17) and (19)–(21) with the well-known diffusion formula (see, e.g., [4,5,13]),

$$J_\mathrm{c}^{(\mathrm{diff})}(\theta) = \frac{3}{8\pi(1 + k_0 l_\mathrm{tr}\theta)^2}\left[1 + \frac{1 - \exp(-2k_0\theta z_0)}{k_0 l_\mathrm{tr}\theta}\right], \quad (z_0 \approx 0.71 l_\mathrm{tr}), \tag{24}$$

which determines the intensity in the close vicinity of the backward direction ($\theta < \lambda/l_\mathrm{tr}$). Equation (24) fails as angle θ of deviation from the backward direction increases. The diffusion formula is applicable as long as the contribution (24) is not exceeded by the nondiffusive contribution (13). So, the diffusion law, $J_\mathrm{c}(\theta) \sim 1/\theta^2$, is changed by $J_\mathrm{c}(\theta) \sim 1/\theta^{(\alpha-2)/(\alpha-1)}$ at angle $\theta \sim \lambda/l_\mathrm{tr}$.

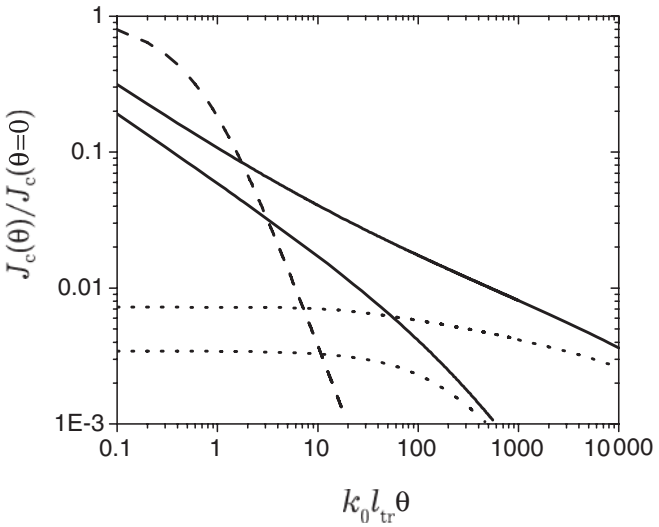

.

FIG. 2. Comparison of different contributions to the intensity of CB. The solid curves are the results of numerical calculations with Eqs. (13)–(15) and Eq. (19), the dashed curve is the diffusion formula (24), and the dotted curves are obtained with the second-order scattering approximation. The lower and upper curves pertain to the scattering phase function (9) with $\alpha = 3$ and $\alpha = 2$, respectively; in both cases, $\langle\cos\vartheta\rangle = 0.9$.

From the results obtained above it follows that the intermediate interval,

$$\frac{\lambda}{l_\mathrm{tr}} < \theta < \frac{\lambda}{\vartheta_0^{\alpha-1} l_\mathrm{tr}} \left(\text{or } \frac{\lambda}{\vartheta_0 l}\right), \tag{25}$$

appears in the angular dependence of the backscattering intensity due to the nondiffusive multiple scattering. This interval gets wider as ϑ_0 decreases. The second-order scattering contribution to the intensity dominates only at large angles $\theta > \lambda/\vartheta_0 l$.

All of the preceding is illustrated by the results of numerical calculations with $\alpha = 3$ and $\alpha = 2$ shown in Fig. 2. For $\alpha = 2$ the nondiffusive contribution to $J_\mathrm{c}(\theta)$ gets higher and intermediate angular interval $\lambda/l_\mathrm{tr} < \theta < \lambda/\vartheta_0 l$ increases as compared to the Henyey-Greenstein case.

IV. COMPARISON WITH EXPERIMENTAL DATA

From the results obtained above it follows that the intensity at the wings of the CB cone ($\theta > \lambda/l_\mathrm{tr}$) is governed by multiple scattering through small angles and single backscattering. Thus the value of intensity is affected by two factors. One factor is the angular dependence of the phase function at relatively small angles. Another factor is the angle-average cross section of backscattering.

For given σ and $\langle\cos\vartheta\rangle$ the backscattering cross section for large Mie particles appears to be great as compared to the power-law phase function (9). This is due to the Glory effect [5]. Therefore, the nondiffusive contribution to the CB intensity can exceed the value calculated with the backscattering cross section (14).

It is of interest to test the validity of our theoretical results by comparing with appropriate experimental data [5].

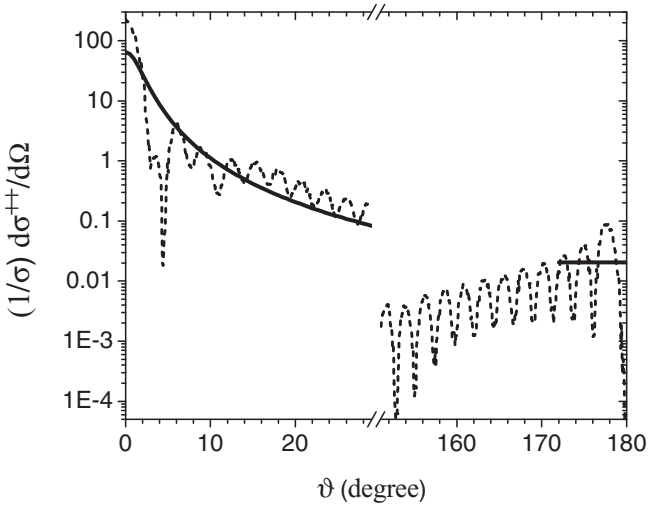

FIG. 3. Normalized differential cross section for circularly polarized light. The dashed curves are the results of calculations [5] for 4.66-μm-radius polystyrene spheres in water (the wavelength of light in water $\lambda = 0.385$ μm, size parameter $k_0 a = 76$). The solid curve at the left is the power-law phase function (9) with $\alpha = 2.5$, $\vartheta_0 = 0.035$. The angle-average cross section of backscattering $\sigma_b^{(++)}/\sigma$ is shown by the horizontal solid line at the right of the figure.

Measurements [5] of the CB cone were carried out for water suspension containing large polystyrene spheres (the particle radius a is about ten times larger than the wavelength of light). The incident beam was circularly polarized, and the backscattered waves with the same polarization were detected. Thus, for quantitative comparison with data [5], the polarization state of light should be taken into account.

In the case being considered we are interested in the intensity of circularly polarized component which is determined by quantity $I_{(++)} = \frac{1}{2}(I + V)$, where I is the total intensity and V is the fourth Stokes parameter [14]. Quantities I and V obey individual transfer equations which differ from each other only by the differential cross sections $d\sigma/d\Omega$ and $d\sigma^{(V)}/d\Omega$ entering into these equations [see, e.g., Eq. (3)] [30]. With allowance for the difference in the cross sections, the CB of light with no change of the circular polarization is described by [31]

$$J_c^{(++)}(\theta) = \tfrac{1}{2}\big[J_c(\theta) + J_c^{(V)}(\theta)\big], \tag{26}$$

where $J_c(\theta)$ is determined by Eq. (4) [or by Eq. (13)] and the value of $J_c^{(V)}(\theta)$ can be obtained from $J_c(\theta)$ by substitution of $d\sigma^{(V)}$ for $d\sigma$.

For large scattering particles, the differential cross sections $d\sigma$ and $d\sigma^{(V)}$ coincide very closely at relatively small angles [30,31]. Therefore, function I_q [see Eq. (5)] that is responsible for the small-angle multiple scattering can be thought to be unaffected by the polarization state of light. This is consistent with the fact that circularly polarized light depolarizes over distances which are much greater than the transport mean free path l_{tr} [30,31].

The difference between the cross sections shows up only at large angles [30] to give the angle-average cross sections of backscattering,

$$\sigma_b = \overline{\frac{d\sigma}{d\Omega}}(-1), \quad \sigma_b^{(V)} = \overline{\frac{d\sigma^{(V)}}{d\Omega}}(-1), \tag{27}$$

that appear, respectively, in Eq. (13) for $J_c(\theta)$ and in an analogous equation for $J_c^{(V)}(\theta)$.

As a result, the intensity $J_c^{(++)}(\theta)$ of CB with no change of the circular polarization can be calculated from Eq. (13) with $\sigma_b^{(++)}$ taken from

$$\sigma_b^{(++)} = \frac{1}{2}\left(\overline{\frac{d\sigma}{d\Omega}}(-1) + \overline{\frac{d\sigma^{(V)}}{d\Omega}}(-1)\right). \tag{28}$$

When comparing our theoretical results with experiment [5] we take advantage of the numerical data for $d\sigma^{(++)} = \frac{1}{2}(d\sigma + d\sigma^{(V)})$ obtained with the Mie theory in [5]. The numerical data for the scattering cross section at relatively small angles ($\vartheta < 30^\circ$) is approximated by the phase function (9) with $\alpha = 2.5$. The value of $\sigma_b^{(++)}$ is determined directly from the numerical calculations [5] of $d\sigma^{(++)}$ (see Fig. 3).

Theoretical and experimental results for the CB intensity are illustrated in Fig. 4.

As follows from Fig. 4, our calculations are in excellent agreement with the experimental data. This means that the wings of the CB cone are governed by the nondiffusive trajectories of wave propagation and are well described within the framework of the approximation proposed above to derive Eqs. (4) and (13). The diffusion theory [see Eq. (24)] appears to be valid within the angular region of the order of the width of the CB cone at half-maximum.

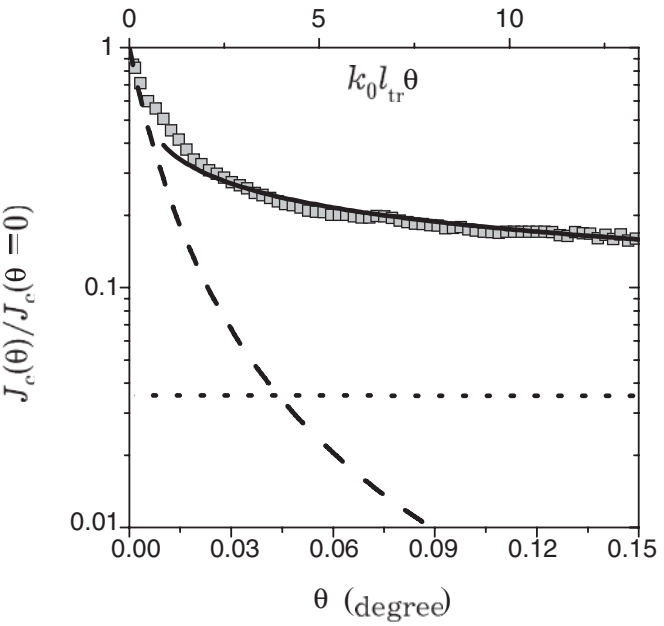

FIG. 4. Intensity of CB from water suspension of 4.66-μm-radius polystyrene microspheres ($l_{tr} = 314$ μm, $l_{tr}/l = 11.36$). The solid curve is the result of Eq. (16) with $\alpha = 2.5$, the dashed curve is the diffusion formula (24), and the dotted curve is the second-order scattering approximation. The squares are experimental data [5].

V. CONCLUSIONS

In conclusion, we have calculated the intensity at the wings of the CB cone and bridged the gap between the results of the diffusion and second-order scattering approximations. Three areas can be distinguished in the angular dependence of the intensity. The regions of diffusive propagation ($\theta < \lambda/l_{\rm tr}$) and second-order scattering ($\theta > \lambda/l\vartheta_0$, ϑ_0 is the characteristic angle of single scattering) are separated by an intermediate region where the wave reflection from the medium results from the forward multiple scattering before and after single deflection through a large angle (of the order of π). As angle θ increases, $\theta > \lambda/l_{\rm tr}$, the diffusion law of the intensity decrease $J_{\rm c}(\theta) \sim 1/\theta^2$ transforms to $J_{\rm c}(\theta) \sim 1/\theta^{\frac{\alpha-2}{\alpha-1}}$, where exponent $\frac{\alpha-2}{\alpha-1}$ depends on the form of the phase function. At rather large angles, $\theta > \lambda/l\vartheta_0$, the intensity decreases with angle θ according to universal law $J_{\rm c}(\theta) \sim 1/\theta$ which follows from the second-order scattering approximation. So, the effect of the phase function on the angular dependence of $J_{\rm c}(\theta)$ reveals itself evidently within interval $\lambda/l_{\rm tr} < \theta < \lambda/l\vartheta_0$.

The results obtained above present a way of estimating the angular dependence of the single-scattering cross section from the measurements of CB wings. This may be useful in studies of multiply scattering media such as colloidal suspensions of large Mie particles, various random media with long-range correlations of inhomogeneities and biological tissues.

ACKNOWLEDGMENTS

The authors thank E. E. Gorodnichev and A. I. Kuzovlev for helpful discussions and valuable advice. We are also grateful to D. S. Uryupina for help in numerical calculations. This work was supported by the Russian Presidential Grants for the Support of the Leading Scientific Schools (Projects No. NSh-3153.2008.2 and No. NSh-64806.2010.2), the Ministry of Education and Science of the Russian Federation (Program for the Development of Science at High School, Project No. 2.1.1/1871), and the International Science and Technology Center (Project No. 3691).

[1] M. Störzer, P. Gross, C. M. Aegerter, and G. Maret, Phys. Rev. Lett. **96**, 063904 (2006).
[2] F. Scheffold and G. Maret, Phys. Rev. Lett. **81**, 5800 (1998).
[3] Y. Kuga and A. Ishimaru, J. Opt. Soc. Am. A **1**, 831 (1984); M. P. Van Albada and A. Lagendijk, Phys. Rev. Lett. **55**, 2692 (1985); P. E. Wolf and G. Maret, *ibid.* **55**, 2696 (1985).
[4] P. E. Wolf, G. Maret, E. Akkermans, and R. Maynard, J. Phys. (France) **49**, 63 (1988); M. B. van der Mark, M. P. van Albada, and A. Lagendijk, Phys. Rev. B **37**, 3575 (1988).
[5] R. Lenke, R. Tweer, and G. Maret, J. Opt. A: Pure Appl. Opt. **4**, 293 (2002).
[6] M. Kaveh, M. Rosenbluh, I. Edrei, and I. Freund, Phys. Rev. Lett. **57**, 2049 (1986).
[7] D. S. Wiersma, M. P. van Albada, B. A. van Tiggelen, and A. Lagendijk, Phys. Rev. Lett. **74**, 4193 (1995).
[8] D. V. Vlasov, L. A. Zubkov, N. V. Orekhova, and V. P. Romanov, JETP Lett. **48**, 91 (1988).
[9] H. K. M. Vithana, L. Asfaw, and D. L. Johnson, Phys. Rev. Lett. **70**, 3561 (1993).
[10] R. Sapienza, S. Mujumdar, C. Cheung, A. G. Yodh, and D. Wiersma, Phys. Rev. Lett. **92**, 033903 (2004).
[11] Y. L. Kim, Y. Liu, V. M. Turzhitsky, H. K. Roy, R. K. Wali, and V. Backman, Opt. Lett. **29**, 1906 (2004); Y. L. Kim, Y. Liu, R. K. Wali, H. K. Roy, and V. Backman, Appl. Opt. **44**, 366 (2005).
[12] Yu. N. Barabanenkov, Izv. Vyssh. Uchebn. Zaved. Radiofiz. **16**, 88 (1973).
[13] M. C. W. van Rossum and Th. M. Nieuwenhuizen, Rev. Mod. Phys. **71**, 313 (1999).
[14] M. I. Mishchenko, L. D. Travis, and A. A. Lacis, *Multiple Scattering of Light by Particles: Radiative Transfer and Coherent Backscattering* (Cambridge University Press, Cambridge, 2006).
[15] K. Muinonen, Waves Random Media **14**, 365 (2004); V. P. Tishkovets and M. I. Mishchenko, J. Quant. Spectrosc. Radiat. Transfer **110**, 139 (2009); M. I. Mishchenko, J. M. Dlugach, and L. Liu, Phys. Rev. A **80**, 053824 (2009).
[16] P. A. de Wolf, IEEE Trans. Antennas Propag. **AP-19**, 254 (1971).
[17] V. Tuchin, L. Wang, and D. Zimnyakov, *Optical Polarization in Biomedical Applications* (Springer, Berlin, 2006).
[18] B. van Tiggelen and H. Stark, Rev. Mod. Phys. **72**, 1017 (2000).
[19] M. V. Berry and I. C. Percival, Opt. Acta **33**, 577 (1986).
[20] V. A. Markel, V. M. Shalaev, E. Y. Poliakov, and T. F. George, J. Opt. Soc. Am. A **14**, 60 (1997).
[21] L. D. Landau, E. M. Lifshitz, and L. P. Pitaevskii, *Electrodynamics of Continuous Media*, 2nd ed. (Pergamon, Oxford, 1984).
[22] A. Ishimaru, *Wave Propagation and Scattering in Random Media* (Academic Press, New York, 1978).
[23] H. C. van de Hulst, *Multiple Light Scattering* (Academic Press, New York, 1980), Vols. 1 and 2.
[24] Y. M. Lure, C. C. Yang, and K. C. Yeh, Radio Sci. **24**, 147 (1989).
[25] D. B. Rogozkin, Laser Phys. **5**, 787 (1995).
[26] V. V. Marinyuk and D. B. Rogozkin, Laser Phys. **19**, 176 (2009).
[27] M. Abramowitz and I. A. Stegun (editors), *Handbook of Mathematical Functions with Formulas, Graphs and Mathematical Tables* (Dover, New York, 1979).
[28] L. Reynolds and N. J. McCormick, J. Opt. Soc. Am. **70**, 1206 (1980).
[29] E. Amic, J. M. Luck, and Th. M. Nieuwenhuizen, J. Phys. A: Math. Gen. **29**, 4915 (1996).
[30] E. E. Gorodnichev, A. I. Kuzovlev, and D. B. Rogozkin, JETP Lett. **68**, 22 (1998); JETP **104**, 319 (2007).
[31] E. E. Gorodnichev, A. I. Kuzovlev, and D. B. Rogozkin, JETP **106**, 731 (2008).